http://mmg.tversu.ru ISSN 2311-1275

MMG *Mathematical Modelling and Geometry*

Volume 4, No 3, p. 31 – 49 (2016)

Orbital Stellar Stereoscopic Observatory Project: Motivation and Autonomous Navigation in the Heliocentric Transfer and Operational Orbits

M. S. Chubey[1,a], **V. V. Kouprianov**[1,2,b], **V. N. L'vov**[1,c], **S. D. Tsekmeister**[1,c], **A. V. Bakholdin**[3,d], **S. V. Markelov**[4,e], and **G. V. Levko**[5,f]

[1] Central (Pulkovo) Astronomical Observatory, Russian Academy of Sciences, 65 Pulkovskoye Ave., Saint Petersburg, 196140, Russia

[2] Department of Physics and Astronomy, University of North Carolina at Chapel Hill, Phillips Hall, 120 E. Cameron Ave., Chapel Hill, NC 27599, USA

[3] Saint Petersburg National Research University of Information Technologies, Mechanics and Optics, 49 Kronverkskiy Pr., Saint Petersburg, 197101, Russia

[4] Special Astrophysical Observatory, Russian Academy of Sciences, Nizhnij Arkhyz, Zelenchukskiy Region, Karachai-Cherkessian Republic, 369167, Russia

[5] Saint Petersburg Research Institute of Television, 22 Politekhnicheskaya St., Saint Petersburg, 194021, Russia

e-mail: [a] mchubey@gao.spb.ru, [b] v.k@bk.ru, [c] epos-gao@mail.ru, [d] bakholdin@aco.ifmo.ru, [e] markel@sao.ru, [f] levgen@mail.ru

Received 21 November 2016, in final form 8 December. Published 9 December 2016.

Abstract. Orbital Stellar Stereoscopic Observatory (OStSO) project is designed for long-term fundamental investigations in astrometry, celestial mechanics, including the asteroid and comet hazard problem, stellar astronomy, and astrophysics. OStSO assumes placing two identical spacecrafts (SC) in the vicinity of L_4 and L_5 Lagrangian libration points of the "Sun – Earth+Moon" system. This configuration has novel features for 3D astronomical observations and monitoring of the solar system events and phenomena. Autonomous space navigation methods are critical for controlling the OStSO deployment, monitoring of the observatory baseline, and for the success of its scientific program. Traditional optical star and Sun sensors have been designed to fit the particular features of the orbital movements and pointing of the main instruments.

Keywords: space project, autonomous space navigation, space instruments, libration centers

PACS numbers: 07.87.+v, 95.10.Ce, 95.10.Eg, 95.55.-n, 95.55.Fw, 96.30.-t

1. Introduction

The "**O**rbital **S**tellar **St**ereoscopic **O**bservatory" (OStSO) project [1] originates from the **I**nterplanetary **S**olar **S**tereoscopic **O**bservatory (ISSO) [2] designed as a long-lasting space stereoscope observatory [3]. Of the two main design options of the ISSO, we present here the "stellar" option for observations of stellar-like and extended objects, focused at solving the problems of astrometry and celestial mechanics [4], including the asteroid and comet hazard (ACH) problem [5], stellar astronomy, and astrophysics [6]. The major technological aspects of creating the ISSO and OStSO have been evaluated in 2007 and 2010 with participation of Lavochkin and Reshetnev corporations' specialists, with a thorough discussion. From these discussions, we have the following conclusions and recommendations:

1. Implementation is possible on the base of the "Navigator" platform on the rocket "Soyuz–2" with the "Frigate" booster;

2. Split the layout into "solar" (ISSO) and "stellar" (OStSO) options. Both options demand a star sensor for navigation and control. The principal differences between these options are:

   (a) their basically different target objects, pointing systems, and programs;

   (b) an extensive and complicated set of solar instruments that should deal with the strong solar radiation flux, which will require the use of special devices for protecting instruments and detectors in the "solar" option;

   (c) only a single astrograph as the main instrument on board is necessary in the "stellar" option.

2. Scientific Objectives and Motivation

The geometric layout of OStSO is shown in Fig. 1.

The five instrumental and scientific arguments to create OStSO in L_4 and L_5 are as follows:

1. Environmental conditions for the on-board equipment are similar and even milder than those near the Earth: strong radiation from van Allen radiation belts and considerable temperature changes while crossings the Earth's shadow are absent.

2. These points are at 1 AU (astronomical unit) from the Sun, so there is no need in developing and testing any extra instrument-protecting systems other than those used for near-Earth orbits.

3. Spatial separation between the Sun–Earth Lagrangian points L_4 and L_5 permits synchronous triangulation observations with the effective baseline of $\sqrt{3}\,AU \approx 259.1$ million km for research in the solar and solar-terrestrial

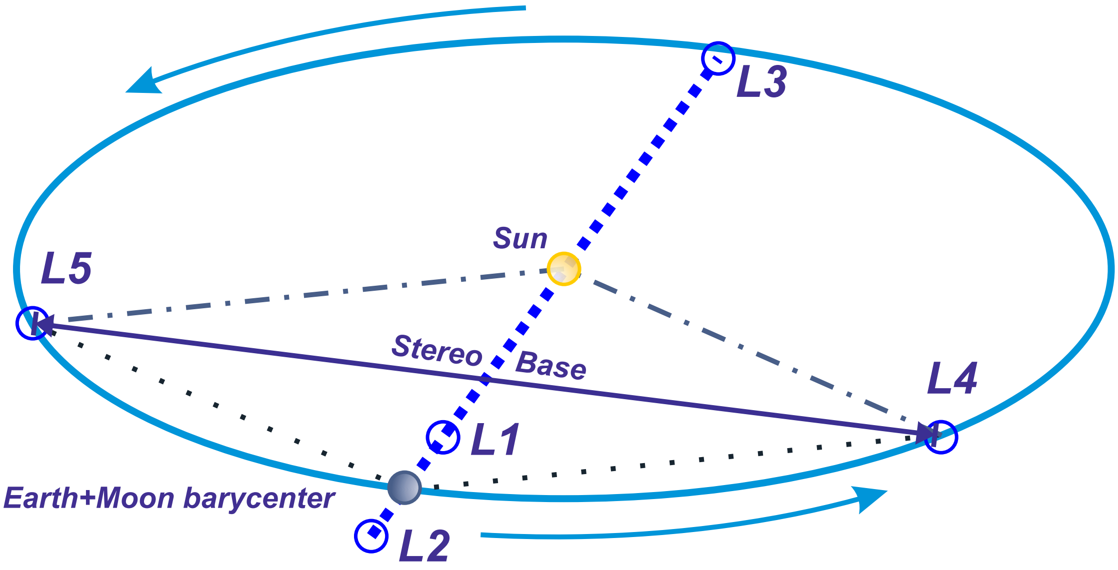

Figure 1: Placement of instruments at Lagrange centers L_4, L_5. Vector connecting stable Lagrange triangle libration centers L_4 and L_5 forms the main baseline of the OStSO. Installing an extra spacecraft in the near-Earth space (for instance, the Euler centers L_1, L_2) would add two more 1 AU baselines.

physics, for solving the problems related to the asteroid and comet impact hazard, as well as for other branches of astronomy as a whole. Beyond any doubts, synchronous astrometric and photometric observations from two points with a wide field of view will provide a very stimulating material for investigations in stellar and galactic astronomy, astrometry, and astrophysics.

4. Physical properties of space in the vicinities of the centers are similar to those in the geostationary orbit, densely occupied since the end of the past century; by any means, these points will be used in the current century due to their convenience for long-term monitoring and research programs in stable conditions, especially for observing the Sun from substantially different directions. Furthermore, they cause no pollution to the near-Earth environment.

5. We support the European vision: the XXI century will concentrate its efforts on the fundamental research of the solar system involving modern technologies.

We solve the following problems in our project:

- installation scenario, tolerances and modeling [7], Fig. 2;
- autonomous navigation with a star sensor [8];
- operational orbit control;

- instrumental, methodical, and design solutions;
- feasibility study for the long-term program.

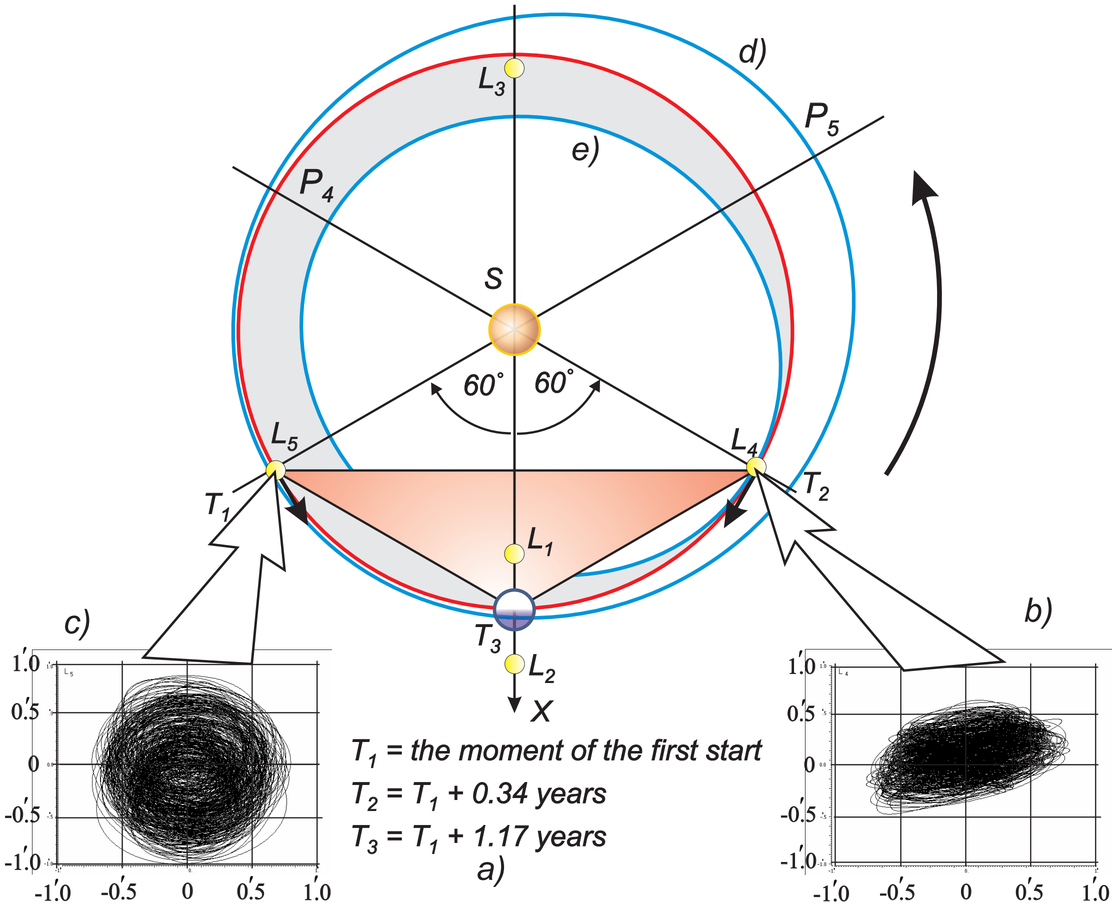

Figure 2: Spatial configuration and deployment to operational orbits near the Lagrangian libration points L_4, L_5 (projected onto the ecliptic plane) for two spacecrafts. T_3 denotes the Earth, and S denotes the Sun. The triangle $L_4L_5T_3$, with vertices always lying in the ecliptic plane is subject to a quasi-solid rotation around the Sun with the period of one year. Inner and outer circles are the calculated one-year Earth–L_5 (d) and Earth–L_4 (e) heliocentric transition orbits. Panel (a) shows the time sequence of spacecraft deployment. Panels (b) and (c) show the enlarged vicinities of the points L_4, L_5 and libration motions of the spacecrafts on the timescale of about 160 years [7]. Extent of these regions is ~ 65000 km, which is about 2.5×10^{-4} of the baseline length B that is subject to eccentric annual variation by 1.7%.

Perspective range for the baseline $L_4 - L_5$ reaches 5 kpc at $\sigma_1 = 0.''0005$ [6]. The solar system objects are in the nearest zone of this range [4]. Tolerances on installation of the spacecrafts are: $\Delta R \leq 1000$ km, $\Delta V \leq 0.1$ m/s, $\Delta L \approx 30000$ km. This provides the stable libration movement during 12 years, the lifetime designed, with amplitude not exceeding 30000 km. Note that the 12-year interval covers a half of the full solar cycle of 22 years.

The main driving idea for our small research group was to facilitate the traditional photographic astronomy methods in orbital conditions with modern instrumentation, enriching them by synchronous 3D vision with such a large stereo base.

Only such problems are included in the scientific program that have evident advantage in the OStSO project as compared to the near-Earth and ground-based observations, i. e. observations from a single direction. The same principle, in a limited way, can be also extended to solar studies.

3. Scientific Program

Scientific program includes the following three principal groups of tasks:

1. *Celestial mechanics and astrometry.* Quasi-synchronous observations of the solar system bodies and the fundamental aspects of the asteroid and comet hazard (ACH) problem, based on high-resolution astrometric and photometric observations. Research in the kinematics of small solar system bodies: near-Earth (NEA) and main-belt asteroids, as well as trans-Neptunian objects (TNOs). OStSO can be used for measuring physical properties and motions of solar system bodies at the distances of up to 2000 AU. This may help one to study the migration of minor bodies into the inner area of the solar system and its influence on the evolution of the solar system.

2. *Stellar astronomy and astrophysics.* Determination of trigonometric parallaxes from synchronous observations of stars at distances of up to 5 kpc. New possibilities will appear in the detection of faint stars down to $V = 24^m$ — both single and in multiple systems — in that zone of perspective thanks to the step-and-steer pointing strategy. More attention can be paid to every exposed area of sky. The method is more accurate than the traditional asynchronous one. All targets of conventional astronomy, including positions and the proper motions of stars and double stars motions, are still covered. Observations with a set of middle-band filters allow one to obtain spectral energy distribution (SED) curves for all objects in the wide field of view. Such observations are vital in solving the various problems of Galactic kinematics and dynamics, in astrometry and astrophysics.

3. *Support for ground-based observations of microlensing* in programs like OGLE, EROS, MACHO (and other transients, including transiting extrasolar planets).

Our understanding of advantages of such an observatory is one of the driving forces of our project. Supplied with the properly chosen instrumentation, with a stable base of 259 million km long, the observatory will be ideal for instant, of the order of exposure time, parallax measurements for all objects in the common field of view of the two SCs within the 5 kpc range, while both the observer and the target can be considered non-moving.

The observatory is designed to be equipped with instruments and accessories that allow us to measure at the diffraction limit; its geometric and photometric resolution is comparable to that of the other modern projects. We suppose to fulfil the work with technologies and methods well elaborated in the ground-based CCD astronomy in the optical range from 0.25 to 1.10 μm, using radiation-resistant imaging equipment, but without any cryogenics and in space version.

4. On-board Equipment

The main OStSO instrument is planned to be implemented using the three-mirror scheme of Tsukanova-Korsch [9, 10, 11]. One of the 40 variants considered is illustrated by scheme in Fig. 3. Such an instrument is to be installed on board of each SC and has the following parameters: aperture $D = 1000$ mm, equivalent focal length $f = 30$ m, CCD mosaic filling a circle $d = 350$ mm in diameter, pixel size 10 μm, field of view FOV $= 40' \times 40'$, overall arrangement dimensions of the instrument $130 \times 150 \times 400\,\mathrm{cm}^3$. Angular pixel size is $0.''07$. Assuming that centroiding accuracy is 0.01 pixel for sources with sufficient signal to noise ratio (SNR), it is possible to achieve the positional accuracy of $\sigma_0 = 0.''0007$ in a single observation. This accuracy is obviously degraded for planetary disks. And surely, statistic can reduce the error by an order of magnitude, if necessary. Exposure time in 120 seconds makes it possible to observe stars down to 25^m.

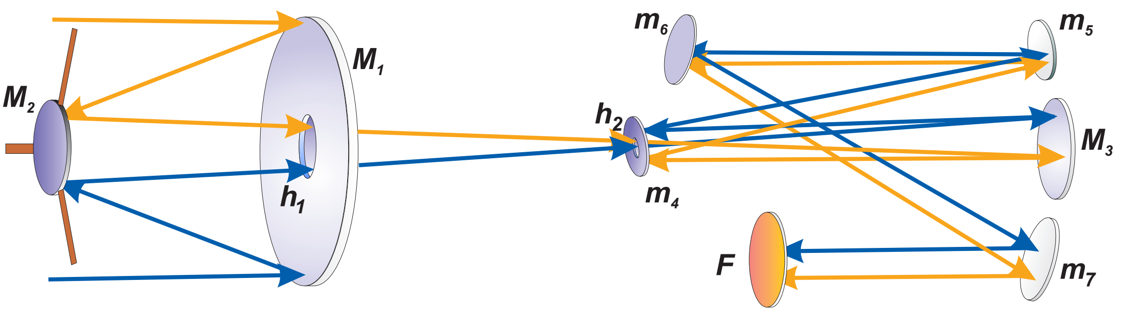

Figure 3: Three-mirror anastigmatic orthoscopic optical system. M_1 and M_3 — ellipsoids, M_2 — hyperboloid, m_{4-7} — planes, F — focal plane with a CCD mosaic. Color filter wheel is placed in front of the detector F.

The telescopes are equipped with identical filters for 10–16 bands covering the spectral range from 0.25 to 1.1 μm. That gives us the opportunity to obtain the averaged energy distribution in the spectra of point and extended objects in the whole FOV.

The “instant” parallax [6] is determined from two synchronous observations of stars in the heliocentric sphere with radius of up to 5 kpc for exposures less than 15 minutes. The uniform observational data obtained during dedicated sky surveys may be helpful in the research of Galactic evolution processes. Color filters will help us to determine the taxonomical classes of asteroids simultaneously with their astrometric and dynamic parameters. The scientific program is compiled keeping in mind the advantages described above and the use of the most efficient conditions of observations in the “meridian” of the OStSO [6]. “Meridian” here stands for the great circle of the celestial sphere generated by its section by the plane which is perpendicular to the OStSO base L_5L_4, Fig. 2, SX is its projection onto the ecliptic.

Two of the possible CCD mosaic schemes in the focal plane F are presented in Fig. 4. Tendency of the growth of the “intellectual facilities” on board is the leading one now. That is why we can include the design of a set of facilities that will be reasonable for platform and the mounting systems.

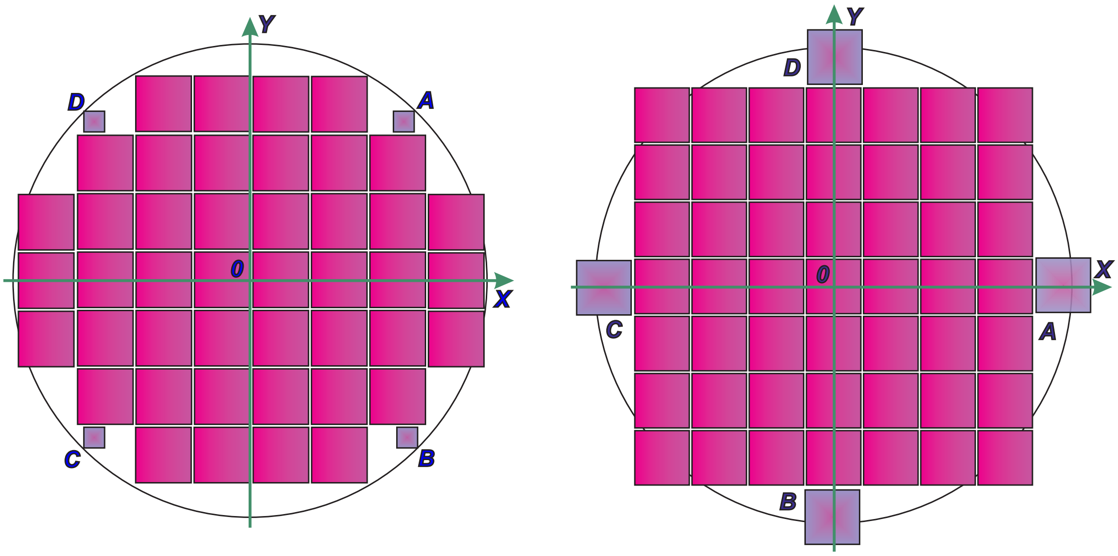

Figure 4: CCD mosaic options: 44 (or 49) p-channel 4K$\times$4K CCDs inscribed into a circle 350 mm in diameter. Every CCD has 2 sections and 4 output nodes with programmed video signal output through any node, for the case of a damage of any register or node element. The p-channeled CCD is more durable than n-channeled one with respect to high-energy particles, and hence a longer lifetime. Given a 10μm pixel, this leads to $\sim$ 0.86 Gigapixels per frame. The A, B, C, D matrices are reserved for guiding and pointing functions: the telescope must not move during the exposure.

The idea of mounting and pointing system is proposed in [12] and is presented in Fig. 5.

The telescope suspension is attached to the support unit of the Navigator platform that is perpendicular both to ecliptic and to the direction to the other conjugate libration point. This suspension is mounted on the C_1 ring. The drive rigidly

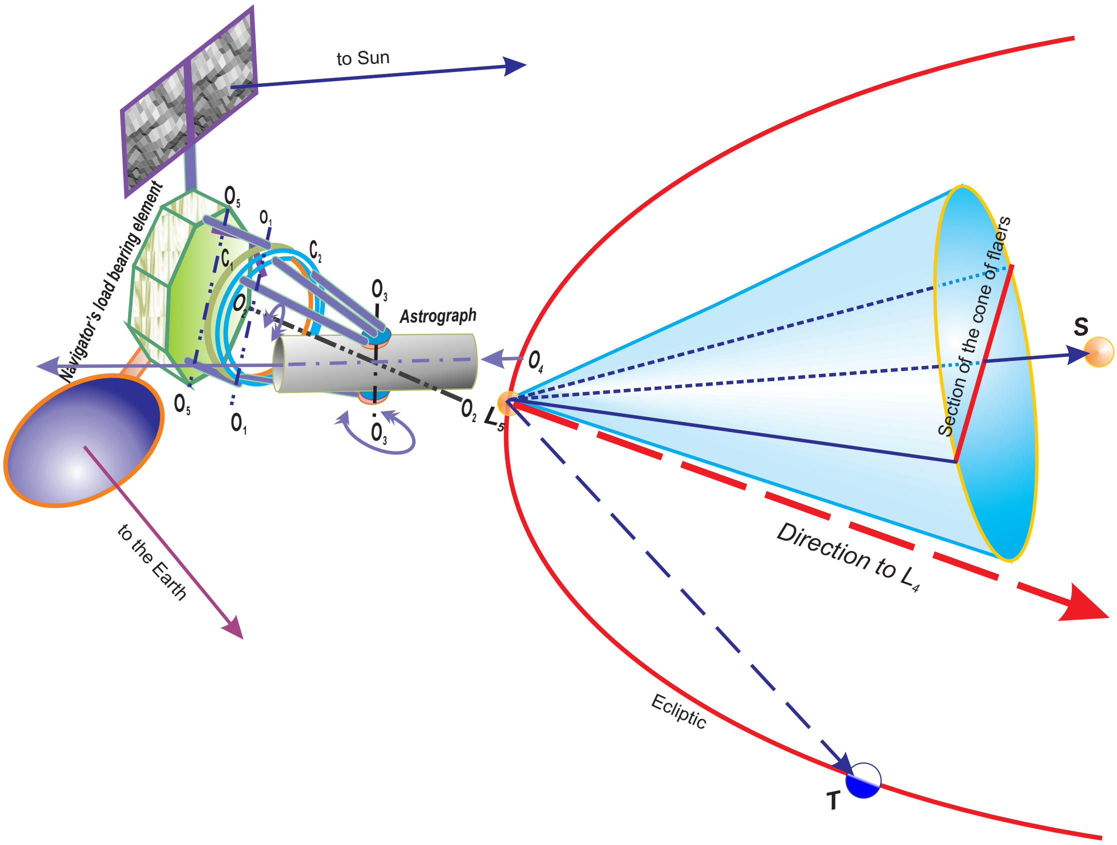

Figure 5: The scheme of mounting and pointing system of astrographs.

coupled to the inner C_2 ring rotates it around the O_2 axis by 360 degrees, rotation being soft in order to prevent vibration. The hard long bars support the telescope suspension that permits rotation around the O_3 axis within the range of $0° - 185°$ from the direction to the associated libration point (in this case, L_4).

Therefore, the pointing system is analogous to that of most of the ground-based telescopes. The only difference is that the whole celestial sphere can be observed. A special tilting mechanism is needed to observe the objects obscured by the platform[12]. Two main modes are supposed to be used: 1) the preferred main mode of synchronous observations in the "meridian" area, with all its advantages; 2) each instrument can work in the single-telescope mode to observe the zones unavailable in the main mode.

The gyroscope system holds the platform so that the solar batteries' normals are constantly oriented towards the Sun, while the radio antenna is oriented towards the Earth. The angle between these directions is very close to $60°$. The bearing platform rotates with the angular velocity of about $1°$/day. These conditions are suitable for a two-step pointing system: coarse pointing with an accuracy of $2' - 5'$ followed by accurate pointing at the target object using the main imaging system.

Automatic procedures for star pattern recognition and determination of object positions in the reference catalog system reliably work for more than three decades. As an example of such work, we may mention the Apex II package [13]. The EPOS software package [14] serves for ephemeris calculations and for modeling of movement of the solar system bodies. Optimized versions of these two Pulkovo programs may be used as the basic tools for on-board SC computers.

5. Star Sensor

To control SC movement along the transfer and operational orbits, planets are to be observed, their coordinates being known from contemporary numerical ephemerides.

The existing autonomous navigational systems mentioned by Mark L. Psiaki and his group are oriented mainly to the near-Earth activities [15, 16]. Similar suggestions by Jo Ryeong Yim and his group [17] and by G. A. Avanesov's group [18, 19] do not solve all problems in the deep space.

For resolving our problems, we need a multi-target highly accurate and all-purpose star sensor. The concept of a two-channel device was presented in [8]. The optimal three-mirror scheme of this sensor known as the "Cook triplet" with two optical elements having non-axial aspheric surfaces is presented in Fig. 6.

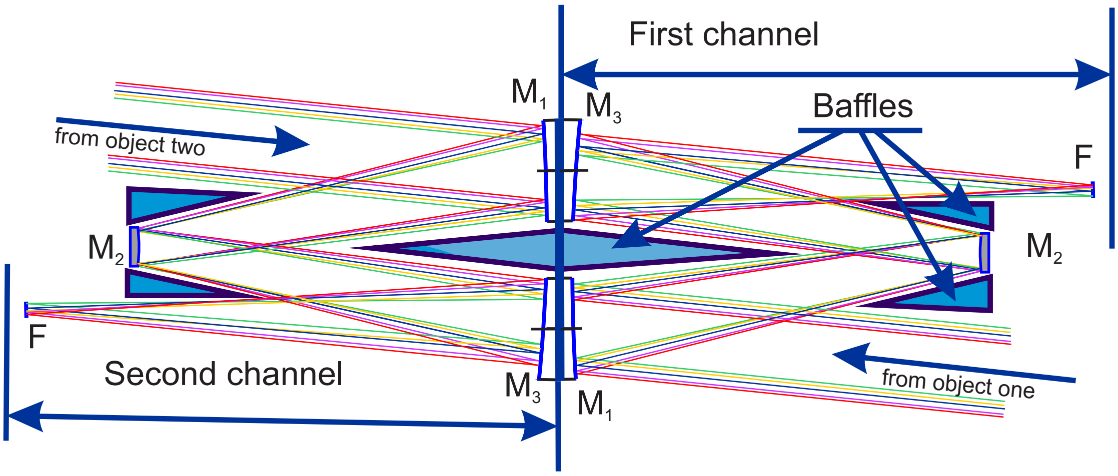

Figure 6: Two-channel star sensor for OStSO optical scheme. $f' = 2500$ mm, $D = 250$ mm, $2\omega = 1°$.

With this sensor, the positions of solar system objects are measured with respect to the stars of a sufficiently dense reference catalog. The parameters of this telescope system are as follows: FOV $2\omega \approx 40' - 60'$, $f \approx 1000 - 2500$ mm, input diameter $D \approx 250$ mm. Maximum distortion along the field is not larger than 0.033%, spectral range is $0.2 - 1\,\mu$m, optical transfer function at the frequency of 100 lines per mm is 0.35. Dissipation circles are less than the Airy disks, and the wave aberrations are less than 0.1λ. This scheme fills a cylindrical volume with radius of 280 mm and length of 1600 mm. A Cardan suspension with a pointing mechanism maintains the autonomous operation of the sensor.

The sensor can obtain two images with different exposure times: the first one contains bright objects — the planets and the Moon, while the other contains faint stars. These frames are then combined by software means. By this procedure, positions of bright extended objects are measured with respect to the faint ones. The scheme of such observations is illustrated in Fig. 7. The angle between the channel axes is equal to 180° with an accuracy of up to a few arcseconds. Shielding is absent, and the limiting magnitude is $V_{\rm lim} \approx 16^m$. The sensor can be deployed after starting acceleration and is introduced to the operational mode to control the transfer orbits.

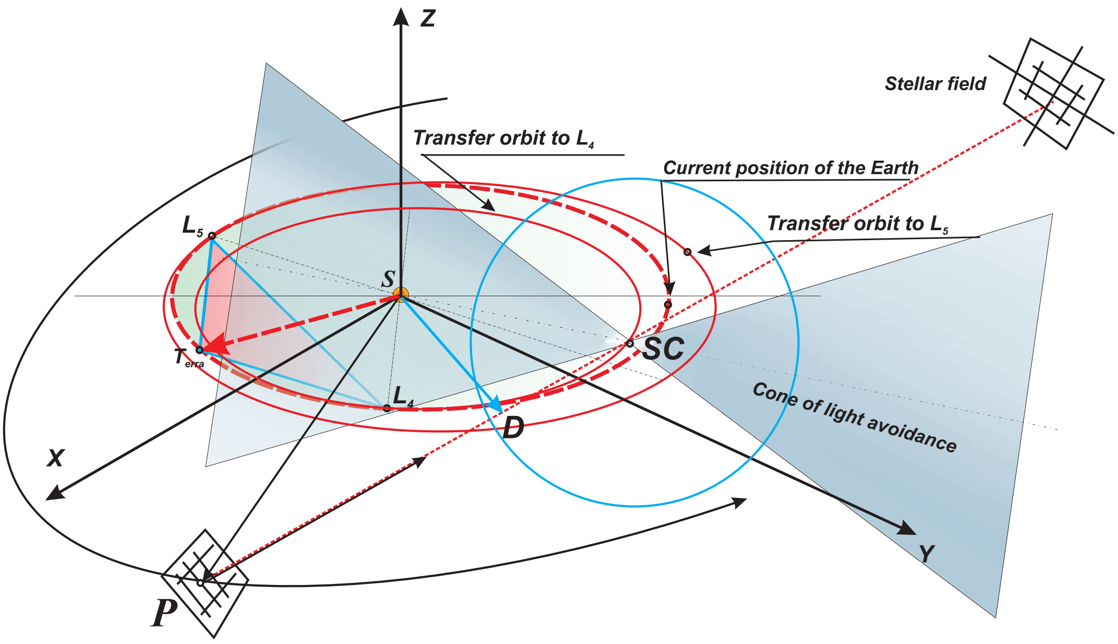

Figure 7: Schematics of a star sensor working on the principle of alignment "P–SC–stellar field". An image of the bright object, a planet with known rectangular coordinates, is on the line PSC. An image of a stellar field with no bright objects gives a reference frame determining the direction SC–P.

It is clearly supposed that, besides astrometric instruments, the following facilities must be installed on board of the SC:

- computer and the clock;
- software for calculations of positions of the solar system objects;
- stellar catalog and software for astrometric and photometric reduction;
- numerical theory of SC motion in the vicinity of libration centers.

The instantaneous remote control mode is impossible here — 1 AU distance is too long for that, and the highest-grade computing equipment must be installed on board.

6. Controlling Directions to Sun and Earth and Platform Orientation

Conditions of the rotational movement of the OStSO with angular velocity of $\sim 1°$/day (Fig. 5) is a good reason for installing a high-resolution solar sensor. Based on the SOHO mission experience [20], it is natural to facilitate a wide-field coronagraph that would in the same time act as a part of the orientation feedback loop and capture synchronous images of the solar vicinity. Surely, we cannot use a ready-made solution, but the principles are already developed and approved: for instance, the SOHO coronographs C1, C2 and C3 by G. E. Brueckner et al. [20, pp. 357–402] can be adapted and used for our purposes mentioned above.

Antenna orientation toward the Earth is maintained using the star sensor, Fig. 6. The whole orientation control feedback loop implies the coordinated work of both sensors.

Both sensors can be used as auxiliary scientific instruments. In the best-case scenario, the solar sensors and coronographs can be used for systematic synchronous observations of the solar activity (SA) events: 83% of the solar surface is observable simultaneously by the two OStSO instruments. The birth, development and decay of the SA processes can be observed during the full heliocycle. In the worst-case scenario, heliographs can provide synchronous observations of SME phenomena, which is critical to the space weather prediction problem. Systematic long-term data from such observations would be of a great value for the more deep and complete understanding of solar physics.

Analogously, systematic observations of the Earth itself as the planet, with the registration of the integral features of the reflected flux, photometrical and spectrophotometrical responses, and finally the space energetic particle distributions and activity in both Lagrangian points — all this can be an extremely valuable observational material in addition to the main scientific goals of the project.

7. Auto-navigation of the Spacecraft

Autonomous navigation in deep space is possible based on observations of two solar system objects that have highly accurate theories of motion. The key notion in this process is a *navigation line*. A spacecraft at the point 1 on the transit orbit, Fig. 8, moving with the velocity of $V \approx 30$ km/s, conducts an observation of the first such line 1–1 with navigation planet Q at a registered moment. After a few minutes, at the point 2, it observes the line 2–2 with the second planet P. And then the observation of the third line 3–3 follows, with the first planet Q. If one assumes the motion of all objects on this timescale as uniform and rectilinear, then the coordinates of the planet Q in lines 1–1 and 3–3 may be averaged and reduced to the moment of observation at the point 2. As a result, we obtain, for this moment, the navigation triangle KPQ, Fig. 8. The observer at point K (that coincides with point 2) will see the planets P and Q on the celestial sphere at the directions KP and KQ, overlaid upon the star background. By simple calculations, we get all angles of the triangle. We also know the lengths of the BP and BQ sides that are the barycentric vectors of planets available from the highly accurate ephemeris. Thus it is possible to derive the BK vector.

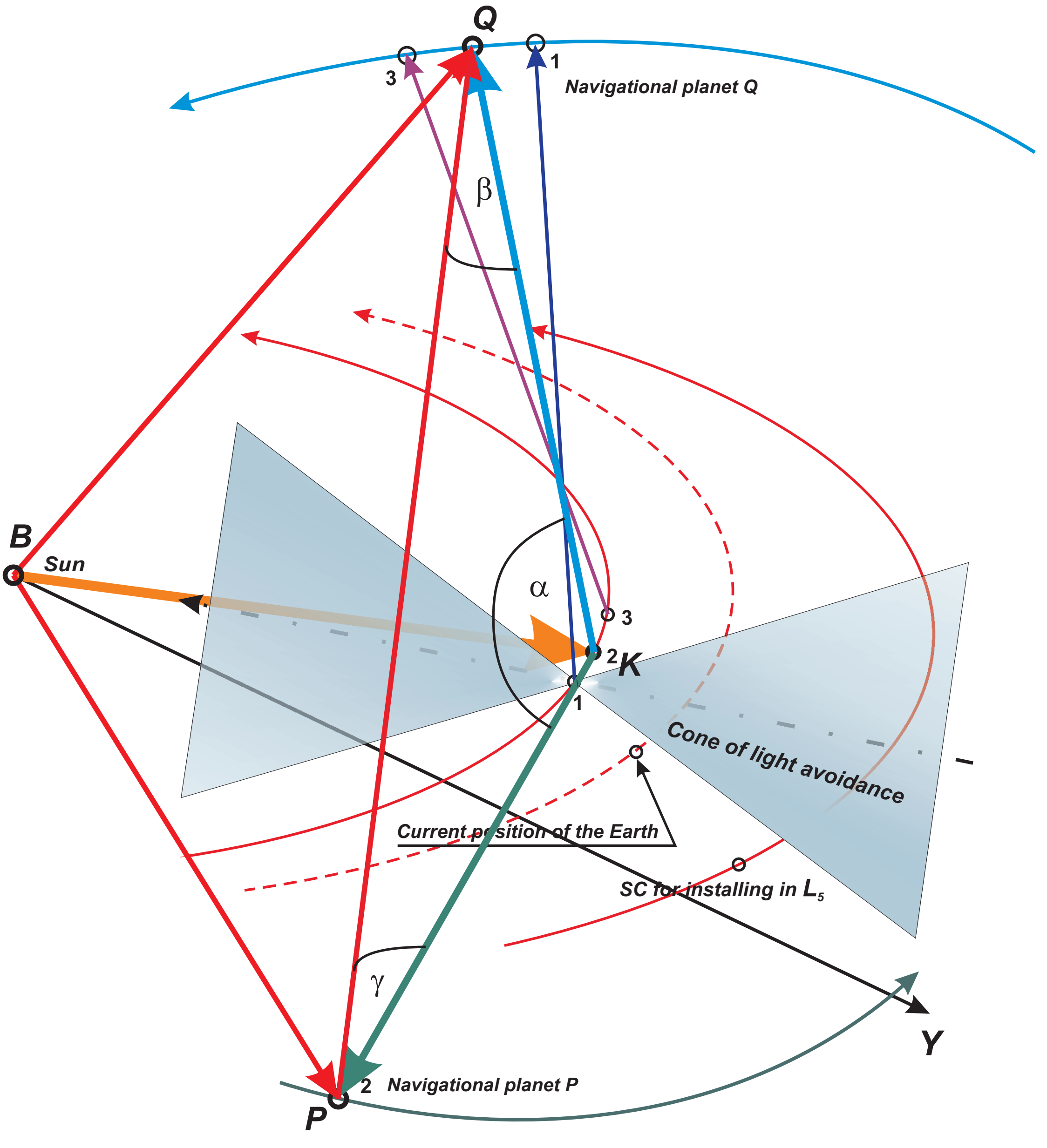

Figure 8: Construction of the triangle PQK by observing planets P and Q at alignments 1–1, 2–2 and 3–3.

Below we present some practical schemes of SC auto-navigation. Using a star sensor, we obtain observations of the two planets reduced to the average moment. Since their spherical coordinates are derived from astrometric reduction of images with reference stars from modern high accuracy catalogs, it is clear that we obtain observer-centric geo-equatorial right ascensions and declinations. The synchronization is provided by the reduction of two observations to one common moment. Let the heliocentric radius vectors of planets and their rectangular coordinates be known: $\vec{r}_1\,(x_1, y_1, z_1)$ and $\vec{r}_2\,(x_2, y_2, z_2)$. Let the above-mentioned right ascensions and declinations be α_1, δ_1 and α_2, δ_2. The direction cosines of the "observer – planet" vectors are

$$l_i = \cos\alpha_i \cos\delta_i,\ m_i = \sin\alpha_i \cos\delta_i,\ i = 1, 2.$$

Heliocentric rectangular coordinates of the spacecraft (x_0, y_0, z_0) may be obtained by the following equations [21]:

$$\begin{aligned} x_0 &= (n_1 l_2 x_1 - n_2 l_1 x_2 - l_1 l_2\,(z_1 - z_2))\,/\,(n_1 l_2 - n_2 l_1)\,, \\ y_0 &= (l_1 m_2 y_1 - l_2 m_1 y_2 - m_1 m_2\,(x_1 - x_2))\,/\,(l_1 m_2 - l_2 m_1)\,, \\ z_0 &= (m_1 n_2 z_1 - m_2 n_1 z_2 - n_1 n_2\,(y_1 - y_2))\,/\,(m_1 n_2 - m_2 n_1)\,. \end{aligned} \tag{1}$$

Astrometric coordinates of each planet α_i, δ_i are derived from the following vectors:

$$\vec{r}_{0_i}(t) = \vec{r}_i\,(t - \tau_i) - \vec{r}_0(t) = \vec{r}_i(t) - \vec{r}_0(t) - \vec{r}_i(t)\tau_i, \tag{2}$$

where $i = 1, 2,\ \tau_i = |\vec{r}_{0_i}|\,/c,\ c$ is speed of light. So we must introduce a light time correction to the vector "SC–planet" obtained from observations. Then the iteration process is used to obtain the solution.

Another navigation scheme deserves noting here as well: optical observation of the Earth is synchronized with the radio signal that arrives from the ground-based station. Then, apart from the equatorial coordinates, we have the time interval τ. Let $\vec{r}_0\,(x_0, y_0, z_0)$ and $\vec{r}_1\,(x_1, y_1, z_1)$ be heliocentric rectangular coordinates of the spacecraft and the Earth, respectively, $l_1 = \cos\alpha_1 \cos\delta_1,\ m_1 = \sin\alpha_1 \cos\delta_1,\ n_1 = \sin\delta_1$ being the direction cosines of the "SC–Earth" vector. In this case, the solution is as follows:

$$x_0 = x_1 - l_1 c\tau,\ y_0 = y_1 - m_1 c\tau,\ z_0 = z_1 - n_1 c\tau. \tag{3}$$

Let us suppose that two observations at the close moments t_B, t_F are sufficient to estimate the SC velocity. Then, for the mean moment $\bar{t}$ and for the values of a function $x\left(\bar{t}\right)$ and its derivative $\dot{x}\left(\bar{t}\right)$, we have

$$\bar{t} = \frac{t_B + t_F}{2},\ x\left(\bar{t}\right) = \frac{x_B + x_F}{2},\ \dot{x}\left(\bar{t}\right) = \frac{x_F - x_B}{t_F - t_B}. \tag{4}$$

The coordinate and velocity vectors obtained may be used as the initial ones for numerical integration of the equations of SC perturbed motion. Any additional statistic will work on the improvement of the orbit accuracy. So we have information on the SC motion in space during the time spans.

If one differentiates the formulae (3) and neglects the errors in Earth position, the total error of the SC vector will be

$$\sigma^2 = c^2\tau^2\left(\sigma_\alpha^2 \cos^2\delta + \sigma_\delta^2\right) + c^2\sigma_\tau^2. \tag{5}$$

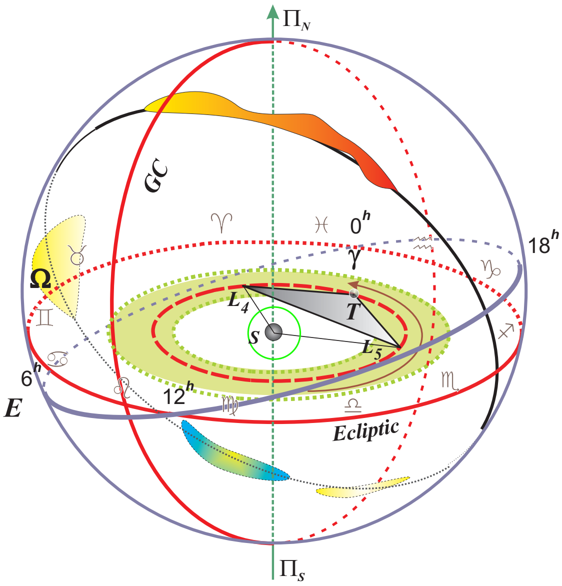

Figure 9: Stereoscopic view of the OStSO.

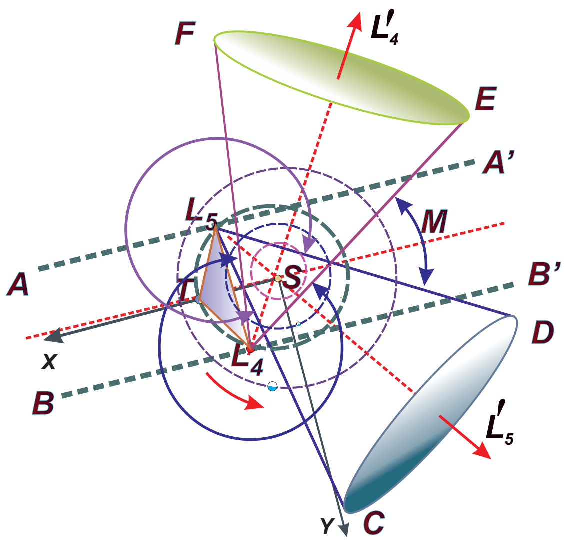

Figure 10: Schematic view of sky zones.

Let $\sigma_\alpha \cos\delta = \sigma_\delta = 0.''001 = 4.85 \cdot 10^{-9}$, $\sigma_\tau = 10^{-4}\,\mathrm{s} = 10^{-9}\,\mathrm{days}$, $c\tau \approx 1$ AU, $c = 173.14\,\mathrm{AU/day}$. Then $\sigma \approx 9.49$ km. The accuracy of the τ value, as it is seen from examining equation (5), is more essential than that of the angular measurements.

It is to be noted that the positional errors will grow proportionally to the separation between navigation planets. So it is hardly reasonable to use the observations of outer planets. But currently it is possible to observe a series of asteroids that have rather accurate theories of motion. All this allows one to determine SC positions with an error of $\sigma \leq 10$ km. This value is enough for the practical autonomous navigation in our case.

As an example, we modeled two sessions of auto-navigation upon the schemes described above for SC moving in the vicinity of libration points of the "Sun – Earth+Moon" system.

The first session (near L_4) represents the synchronous observations of two planets at two moments 2016 January 3 $1^{\mathrm{h}}00^{\mathrm{m}}$ and $1^{\mathrm{h}}10^{\mathrm{m}}$, as per Fig. 8. Using the EPOS software package, observer-centric astrometric right ascensions and declinations of the Earth and Mars were calculated. These values, along with DE405 numerical ephemeris data, were used to calculate heliocentric SC vectors of coordinates and velocities for the mean moment. The discrepancies with the predefined values were 3.2 km in position and 0.0036 km/s in velocity.

The second session (near L_5) represents the observations of the Earth synchronized with the radio signal at two moments 2015 January 1 $0^{\mathrm{h}}05^{\mathrm{m}}$ and $0^{\mathrm{h}}15^{\mathrm{m}}$. It was supposed that only one direction was observed from SC, namely "$SC \rightarrow$ current position of the Earth T", Fig. 7. The observational data: space orientation of the vector "$T \rightarrow SC$" and the interval of time τ, along with the radius vector of the

Earth from the DE405 numerical ephemeris values have been used for calculation of SC heliocentric vectors of coordinates and velocities for the mean moment. The discrepancies with the predefined values were 2.5 km in position and 0.0022 km/s in velocity.

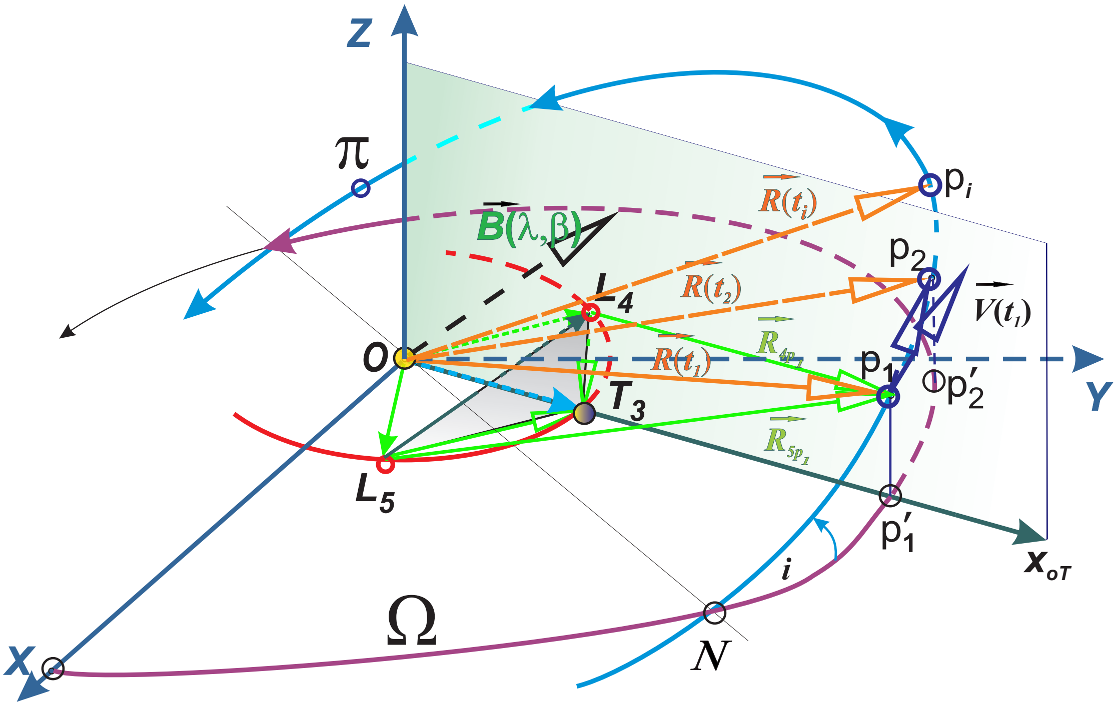

Figure 11: Synchronous observation of a solar system body.

8. Observational Strategy and Scientific Background

The general scheme of the OStSO is shown in Fig. 9. Most accurate positional measurements in stereo mode are obtained within the band around the "meridian" of the OStSO — a section of the celestial sphere by the GC plane that is perpendicular to main base L_4L_5. Separation of the SC positions from the ST line makes it possible to observe the full surrounding space excluding only a Sun-centered sphere of radius equal to half of the Venus orbit size, Fig. 10.

Any synchronous observation allows to directly determine the barycentric radius vector $\vec{R}\,(t_i)$ of the solar system body p_i at the moment t_i, Fig. 11. A series of n radius vectors generates the system of vectorial equations

$$\begin{aligned} \vec{R}_i\,(t_i) &= \vec{R}_0\,(t_0) + \vec{V}_0\,(t_i - t_0) + \delta\vec{R}_i, \\ \left[\delta\vec{R}_i\right] &= 0,\ i = 1, 2, \ldots, n, \end{aligned} \tag{6}$$

where $\delta\vec{R}_i$ is a random error vector with zero mean. A conventional least-squares solution gives the barycentric radius and velocity vectors:

$$\begin{aligned} \vec{R}_0\,(t_0) &= (R_x, R_y, R_z)\,, \\ \vec{V}_0\,(t_0) &= (V_x, V_y, V_z)\,, \end{aligned} \tag{7}$$

which is equivalent to 6 orbital elements, but with an increased accuracy.

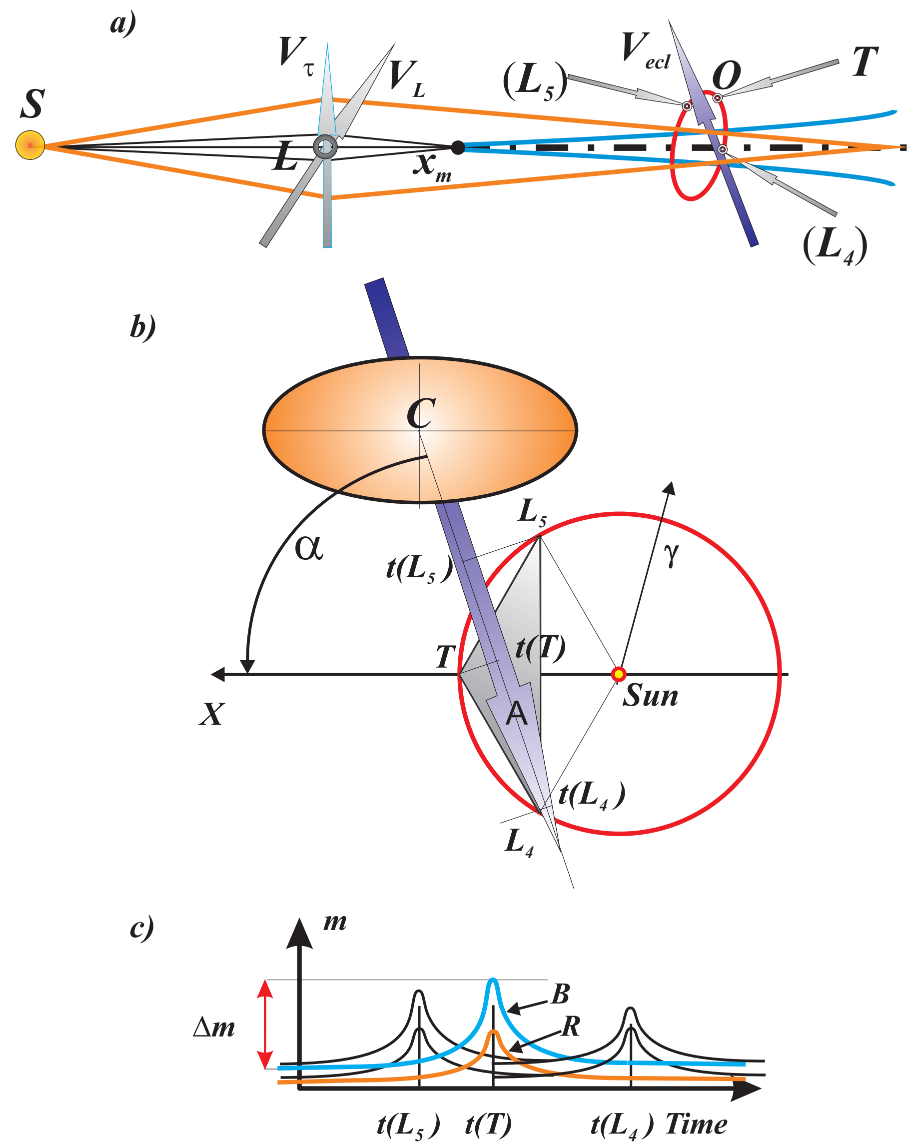

Figure 12: Schematic of microlensing observations. S is lensed and L is lensing objects, (a) The image C of S in the ecliptic O will be comparable in size with the size of the Earth orbit, and, during the transit, will be observed by instruments at L_5, then on Earth T, and finally at L_4. (b) The resulting lightcurve (c) confirms the lensing event and helps to obtain the characteristics of space around objects S and L (see [22, 23, 24]).

An obvious extension of this synchronous observation scheme leads to the "instantaneous" star parallaxes. Their system will differ from the classical one, which is based on the observations by a single instrument over many years from the opposite points of the Earth orbit. Parallaxes of the Gaia mission are performing now on the same classical method in the scanning mode.

Of a particular interest are microlensing observations in accordance with the scheme in Fig. 12.

Our method might be used to verify the Gaia results. As a means to support of the traditional ground-based programs as EROS, MACHO, OStSO microlensing observations increase the accuracy and provide independent confirmation of these events.

9. Conclusions

The OStSO project presented here has been thoroughly worked out in its theoretical aspects and instrumentation design solutions, was presented at conferences, published in journals, and received an approval from the professional community. Our small team is ready to write the technical documentation in collaboration with SC designers. The proposed space-based observatory is efficient in solving problems of ACH and kinematics and dynamics of solar system bodies, as well as many current problems of astrometry, stellar astronomy and astrophysics.

The instruments and methods of autonomous navigation of the OStSO project provide an acceptable accuracy of determination of the spacecraft position and velocity to support the scientific goals of the project. Still it demands for a more powerful artificial intelligence on board and reliability of the signal reception and transfer system that needs to handle a large amount of scientific and telemetry information.

The star sensor developed for this project may be used not only for navigation tasks but also for Earth studies from the distance of 1 AU. The same is valid concerning the solar sensor and heliograph.

Acknowledgements. We express our deep gratitude to Professor V. N. Pochukaev from Mission Control Center in Korolev and to leader of Special Astrophysical Observatory in Zelenchuk region corresponding member of RAS Yu. Yu. Balega with his colleagues for creative discussions and support of our work.

References

[1] Chubey M. S., Grigoriev V. M., Eroshkin G. I., L'vov V. N., Papushev P. G., and Yagudin L. I. *Stereoscopic Principle in Space Observatory.* Kinematics and Physics of Celestial Bodies. 2005, Suppl. No. 5, pp. 172–175

[2] Grigoriev V. M., Papushev P. G., Chuprakov S. A., Chubey M. S., Kulagin E. S., Eroshkin G. I., L'vov V. N., Tolchel'nikova S. A., and Yagudin L. I. *Interplanetary Solar Stereoscopic Observatory.* J. Opt. Technol. 2006, **73**, pp. 251–255

[3] Grigoriev V., Papushev P., Chuprakov S., Chubey M., Eroshkin G., L'vov V., and Pashkevich V. *On the Long-life Solar Stereoscopic Observatory.* Abst. XXV IAU GA, Sydney, Jul 13-26 2003 No. 1371, p. 182

[4] Abalakin V., Chubey M., Eroshkin G., and Kopylov I. *Triangulation Measurements in the Solar System.* Proc. IAU Coll. 180. (Kenneth J. Johnston et al. eds) USNO, Wash. DC, USA, 2000, pp. 132–163

[5] Chubey M. S., Yagudin L. I., L'vov V. N., Tsekmejster S. D., Kouprianov V. V., Eroshkin G. I., Smirnov E. A., and Petrov A. V. *Solving of the ACH Problem in the Project "Interplanetary Solar Stereoscopic Observatory".* Proc. Intl. Conf. ACH–2009 (A. M. Finkelstein, W. F. Huebner, and V. A. Shor, eds.), Saint-Petersburg, "Nauka", 2010, pp. 110–115

[6] Chubey M. S., Kouprianov V. V., L'vov V. N., Markelov S. V., Bakholdin A. V., and Tsukanova G. I. *Solving Stellar Astronomy Problems in the Orbital Stellar Stereoscopic Observatory Project.* Baltic Astronomy. 2014, **24**, pp. 84–91

[7] Chubey M. S., Eroshkin G. I., and Pashkevich V. V. *Space Stereoscopic Observatory Project.* J. Math. Sci. 2005, **128**, No. 2, pp. 2721–2725

[8] Chubey M. S., Koval'chuk L. V., Yes'kov D. N., Seregin D. A., Miloradov A. B., and Kholodova S. I. *Star sensor for the autonomous navigation in the far space.* J. Opt. Technol. 2007, **74**, No. 2, pp. 40–48

[9] Tikhomirova G. I. *Three mirror astronomical lenses.* Izv. Vuzov. Instrumentation. 1967, **10**, No. 12, pp. 70–75 (in Russian)

[10] Korsch D. *Anastigmatic three-mirror telescope.* Appl. Opt. 1977. No. 8, pp. 2074–2077

[11] Chubey M. S., Tsukanova G. I., and Bakholdin A. V. *Specific of the astrograph optical system design for for the Interplanetary Solar Stereoscopic Observatory.* J. Opt. Technol. 2007, **74**, No. 7, pp. 37–41

[12] Chubey M. S., Bakholdin A. V., Kouprianov V. V., Levko G. V., L'vov V. N., Markelov S. V., Tsekmeister S. D., and Tsukanova G. I. *On the pointing system in the "Orbital Stellar Stereoscopic Observatory" project.* Proc. Conf. "Modern problems of the orientation and navigation of spacecrafts". Tarusa, September 8–13, 2014, Space Researches Institute of RAS. Moscow, 2015, pp. 85–94 (in Russian)

[13] Devyatkin A. V., Gorshanov D. L., Kouprianov V. V., and Verestchagina I. A. *Apex I and Apex II software packages for the reduction of astronomical CCD observations.* Sol. Sys. Res. 2010, **44**, No. 1, pp. 68–80

[14] L'vov V. N. and Tsekmeister S. D. *The Use of the EPOS Software Package for Research of the Solar System Objects.* Sol. Sys. Res. 2012, **46**, No. 2, pp. 177–179

[15] Psiaki M. L. *Autonomous orbit and magnetic field determination using magnetometer and star sensor data.* J. Guid. Contr. Dyn. 1995, **18**, No. 3, pp. 584–592

[16] Psiaki M. L. *Autonomous low-earth-orbit determination from magnetometer and sun sensor data.* J. Guid. Contr. Dyn. 1999, **22**, pp. 296–304

[17] Yim J.-R., Crassidisy J. L., and Junkins J. L. *Autonomous Orbit Navigation of Inter-planetary Spacecraft.* American Institute of Aeronautics and Astronautics Paper, 2000, 3936

[18] Avanesov G. A., Bessonov R. V., and Dement'yev V. Yu. *Results of Testing of the BOKZ-M60/1000 star sensor software on a dynamical testbed.* Proc. III All-Russian Conf. "Contemporary Problems of Orientation and Navigation of Spacecrafts", Space Research Institute of RAS, Moscow, 2013, pp. 169–179 (in Russian)

[19] Avanesov G. A., Bessonov R. V., Dement'yev V. Yu., and Mysnik E. A. *Results of Real-world Testing of the BOKZ-M60/1000 Star Sensor.* Proc. III All-Russian Conf. "Contemporary Problems of Orientation and Navigation of Spacecrafts", Space Research Institute of RAS, Moscow, 2013, pp. 180–189 (in Russian)

[20] *The SOHO mission.* Ed. by B. Fleck, V. Domingo, and A. Poland. Kluwer Academic Publishers, 1995

[21] Chubey M. S., L'vov V. N., and Yagidin L. I. *The accuracy estimation of the astrometric measurements in the situation of space stereoscopic observatory.* Fourth Polyakhov Readings. Selected works. Saint-Petersburg, VVM. 2006, pp. 288–295 (in Russian)

[22] Paczynski B. *Gravitational microlensing by the galactic halo.* ApJ 1986, **304**, pp. 1–5

[23] Gould A. *Proper motions of MACHOs.* ApJ 1994, **421**, No. 2, pp. L71–L74

[24] Gould A. *MACHO velocities from satellite-based parallaxes.* ApJ 1994, **421**, No. 2, pp. L75–L78